INTERNATIONAL JOURNAL OF AUTOMOTIVE SCIENCE AND TECHNOLOGY

2024, VOL. 8, NO:4, 467-475 www.ijastech.org e-ISSN: 2587-0963

Effect of Cooling Parameters on In-Mold Flow Behavior in the Microinjection Molding of Piezoelectric Pumps

Fuat Tan[1*], Ahmet Kerem Alkan[1]

[1]*Department of Mechanical Engineering, Faculty of Engineering, Balikesir University, Balıkesir, 10145, Turkey*

Abstract

In this study, the analysis of piezoelectric pumps produced by microinjection was conducted in a computational setting. Using the Face-Centered Cubic (FCC) design of experiments approach, this analysis examined in detail how cooling water temperature and Reynolds number impact product quality and production performance. With cooling water inlet temperatures between 20°C and 30°C and Reynolds numbers from 8000 to 12000, several critical quality parameters were analyzed, including fill time, injection pressure, wall shear stress, sink mark depth, volumetric shrinkage and residual deformation. The results showed that maintaining injection pressure between 113.8 and 116.1 MPa supported effective mold filling, while wall shear stress values between 0.2566 and 0.2617 MPa preserved mold longevity and enhanced surface quality. Volumetric shrinkage held at 2.775% improved dimensional accuracy and product stability, and controlling sink mark depth between 0.2995 and 0.2999 mm minimized surface deformation. Additionally, an optimized fill time of 0.3327 seconds ensured consistent temperature distribution during filling, enhancing overall fill quality. These findings illustrate that by optimizing cooling parameters and flow control, high-quality, dimensionally accurate piezoelectric pumps can be manufactured via microinjection. This study provides a comprehensive methodology to improve both production efficiency and product quality. Furthermore, the presented data will serve as a valuable guide for researchers in the production of piezoelectric pumps using the microinjection molding method.

Keywords: Cooling; Microinjection Molding; Piezoelectric Pump; Warpage

Research Article

History
Received 14.10.2024
Revised 13.11.2024
Accepted 13.12.2024

Contact
* Corresponding author
Fuat TAN
fuattan@balikesir.edu.tr
Address: Mechanical Engineering Department, Faculty of Engineering, Balikesir University, Balikesir, Turkey
Tel: +902666121194

***To cite this paper*:** Tan, F., Alkan A.K. Effect of Cooling Parameters on In-Mold Flow Behavior in the Microinjection Molding of Piezoelectric Pumps. International Journal of Automotive Science and Technology. 2024; 8 (4): 467-475. http://dx.doi.org/10.29228/ijastech..1566495

1. Introduction

With advancements in microinjection molding machines during the 1990s, thermoplastics found applications in various microstructures, including microfluidics, micro-optics, microchips, and medical devices [1]. Certain plastics remain challenging to process in injection molding, highlighting the need for continuous advancements in the technique [2]. The emergence of new nanocomposites has further elevated the importance of microinjection molding [3]. Design of Experiments (DOE) methods can be effectively utilized to determine the quality parameters of products obtained through microinjection molding [4]. Additionally, analyzing the morphology of microinjection-molded samples provides valuable insights into their thermomechanical history [5]. Plastics used in piezoelectric pumps are commonly applied in microelectronic cooling systems, miniature devices and chemical and biological analysis due to their ability to convert mechanical energy into electrical energy [6-8]. The automotive industry is one of the primary sectors harnessing piezoelectric technology. From fuel atomizers and keyless entry systems to seatbelt alerts, airbag and airflow sensors, audible alarms, knock sensors and tire pressure sensors, piezoelectric materials play a crucial role in enhancing vehicle functionality and safety across a wide range of applications [9].

Micro pump production has been successfully developed on surfaces like glass and silicon [10], as well as using polymer materials such as polymethyl methacrylate [11], polydimethylsiloxane [12] and SU-8 photoresist [13]. Injection molding, as a large-scale production method, is considered highly efficient in terms of cost and energy [14]. Consequently, integrating polymer and micro technologies offers potential for new sensor and actuator applications, including fully embedded, low-cost sensors. Toward this goal, piezoelectric polymer materials have been integrated with microinjection-molded components [15]. Various piezoelectric materials include ceramics, ferroelectric polymers [16], polymer-ceramic composites [17] and novel cellular polymers [18]. Wu-lin Chen simulated the injection molding process in mold flow, designed

an experiment based on response surface methodology and identified process parameters that minimized volumetric shrinkage and warpage [19].

H.K. Lee and colleagues examined residual stress distribution and surface replication in polymers, verifying residual stress through photoelastic methods and surface replication conditions [20]. In a study by Guojian Zheng et al., an automotive triangular cover was selected and the Taguchi experimental method was used to determine the effects of processing parameters. An L27 (3^13) orthogonal array was created to evaluate the significance of factors such as mold temperature, melt temperature, injection time, V/P transition, packing pressure and packing time. Ideal warpage levels were achieved using computer-aided engineering software [21]. In the simulation process, µIM experiments are crucial for obtaining accurate data and precision. They provide insights into real processing conditions [22]. Volumetric shrinkage during the injection molding process poses a significant quality challenge. To address this, Hsueh-Lin Wu and Ya-Hui Wang conducted studies aimed at minimizing the volumetric shrinkage in chair bases [23]. Mold design plays a crucial role in managing shrinkage, with parameters often optimized through computer simulations, mathematical modeling [24] and by accounting for raw material viscosity and mold rheology [25].

Cooling these molds is complex; thermodynamic and hydrodynamic calculations are essential for improving mold quality, driving intensive research on conformal cooling channels [26]. Zheng Min Huang and colleagues explored the injection molding of a composite automotive wheel, using simulations to assess filling time, mechanical properties and warpage [27]. Other automotive components such as rear door panels [28], interior parts [29], inner door handles [30], complex door structures [31] and composite engine blocks are also developed through injection molding and simulation for continual performance enhancements [32]. A comprehensive review of the literature indicates an absence of studies directly addressing the production quality and parameter optimization of piezoelectric pumps within the context of plastic injection molding and tooling.

This research makes a significant contribution by precisely and simultaneously optimizing the effects of cooling water temperature and Reynolds number on critical quality parameters such as filling time, injection pressure and surface deformation, with a particular focus on piezoelectric pumps and microinjection processes. By offering a detailed analysis of production efficiency, this study bridges a crucial gap in the literature and provides foundational data to advance both academic understanding and industrial applications in this field.

This study presents a computational analysis of piezoelectric pumps manufactured through microinjection. Employing the Face-Centered Cubic (FCC) design of experiments, the analysis provides an in-depth examination of how cooling water temperature and Reynolds number affect product quality and manufacturing efficiency.

2. Materials and Methods

In recent years, polyoxymethylene (POM) thermoplastic has become a preferred choice for piezoelectric materials, particularly in applications requiring microelectronic cooling and high-precision biomedical technologies. As a semi-crystalline thermoplastic, POM is distinguished by its high structural strength, fatigue resistance, stiffness and cost-effectiveness. The material properties of POM specified for injection analysis are shown in Table 1.

Table 1. POM physical properties

Physical Properties	Value	Unit
Melt density	1.2548	g/cm^3
Melt temperature	210	C
Solid density	1.5285	g/cm^3
Surface temperature	70	C
Elastic modulus (E1)	2900	MPA
Possoins ratio (v12)	0.39	-
Shear moduls	1043	MPA
Maximum shear stress	0.45	MPA
Maximum shear rate	40000	$1/s$

The injection molding process's high temperature and pressure requirements, along with specific experimental design parameters, make it essential to accurately define the material's viscoelastic properties (Figures 1 and 2).

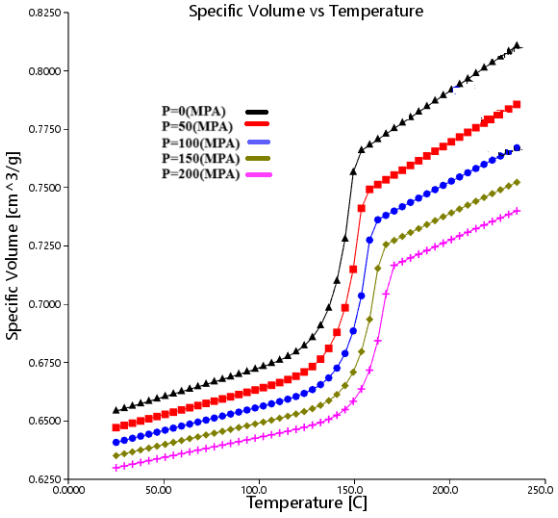

Fig. 1. Specific volume vs temperature of POM material

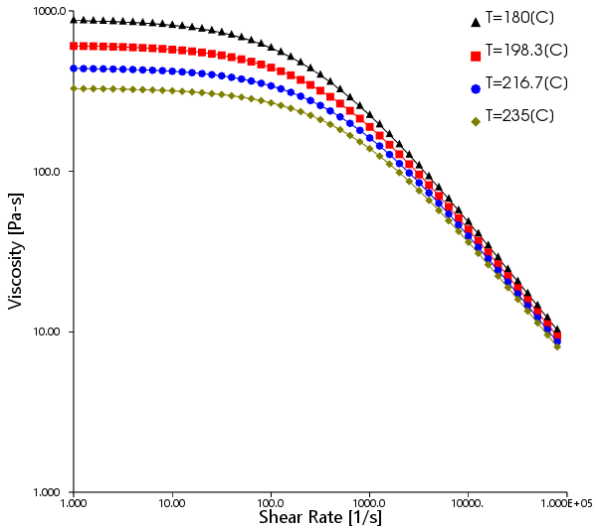

Fig. 2. Viscosity vs shear rate of POM material

The in-mold flow simulation central to this study was performed using the Autodesk Moldflow Insight 2016 version software package and i5 Core processor. This analysis utilized the comprehensive Cool (FEM)-Fill-Pack-Warpage module, which includes both cooling and mold design aspects. The following conservation equations were used to examine the flow behavior in the analyses conducted;

$$\frac{\partial \rho}{\partial t} + \frac{\partial \rho u}{\partial x} + \frac{\partial \rho v}{\partial y} + \frac{\partial \rho w}{\partial z} = 0 \quad (1)$$

The momentum conservation equation:

$$\frac{\partial \rho}{\partial t} + \vec{V}.(\rho \vec{V}) = \frac{\partial \rho}{\partial t} + \vec{V}.\vec{V}\rho + \rho \nabla.\vec{V} = 0 \quad (2)$$

The energy conservation equation:

$$P c_v \frac{dt}{dt} = k\nabla^2 T + \emptyset \quad (3)$$

3. Computational Domain

3.1 Model and mesh

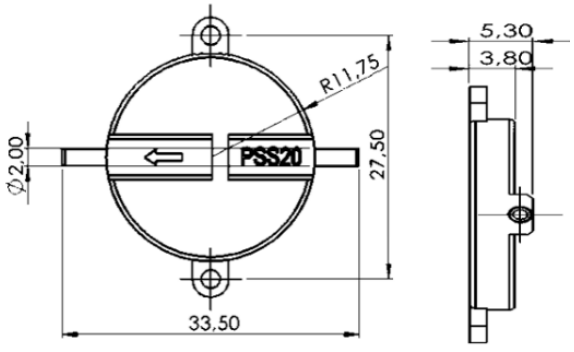

Fig. 3. Model dimensions

The technical drawing dimensions of the model are provided in Figure 3. The piezoelectric solid model used has a core radius of 11.75 mm, an outer width of 33.5 mm and a height of 27.5 mm. The arms extending from both sides have a diameter of 2 mm and the thickest section of the model (side view) measures 5.30 mm.

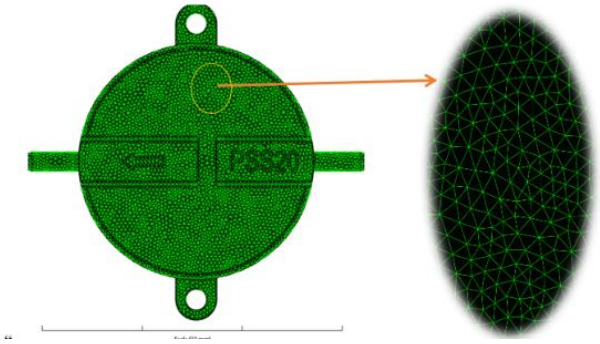

Fig. 4. Mesh structure of the model

Triangles mesh elements were used for the mesh structure, with a single piezoelectric solid model consisting of 24,598 mesh elements and 12,297 nodes. The average aspect ratio is 1.54 (Figure 4).

3.2. Gate Location

A suitability analysis was conducted to ensure that the molten plastic fills the mold from the optimal point with minimal flow resistance, achieving a uniform distribution. This approach is essential for minimizing quality issues such as warpage and volumetric shrinkage. The results of the Gating Suitability and Flow Resistance Indicator analyses are presented in Figure 5.

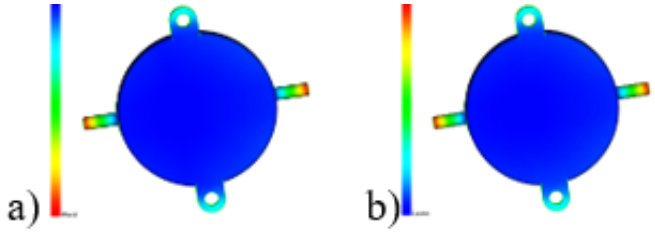

Fig. 5. (a) Gating suitability (b) Flow resistance indicator

3.3 Cooling circuit

To enhance injection production time and product quality, the cooling circuit design employs optimized horizontal channels. Since the process involves molding eight units simultaneously, channel diameters and positioning were carefully selected to ensure fast, uniform cooling, effective temperature control and dimensional stability. The design specifications for the cooling channels are shown in Table 2.

Table 2. Cooling circuit design values

Part dimension (X-axis) (mm)	70.6
Part dimension (Y-axis) (mm)	94.8
Part dimension (Z-axis) (mm)	33.52
Channel diameter (mm)	10
Top and bottom distance (mm)	25
Alignment shape of the circuit with the part	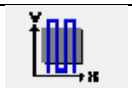
Number of channels per part	2
Distance between channel centers (mm)	30
Distance from part edge (mm)	45

The channel layout according to these design specifications is illustrated in Figure 6.

Fig. 6. Cooling circuit model

3.4 Runner system

The runner system design has a direct influence on fill time and surface quality. To ensure that the molten plastic flows into the mold at optimal speed, temperature and pressure, the runner system was tailored with these factors in mind, enabling the simultaneous production of eight piezoelectric solid models. The optimized runner system design, based on flow rate analysis, is illustrated in Figure 7.

Fig. 7. Runner system design for high-volume production

The results of the flow rate analysis conducted to ensure optimal flow rate control in the runner system are shown below (Figure 8).

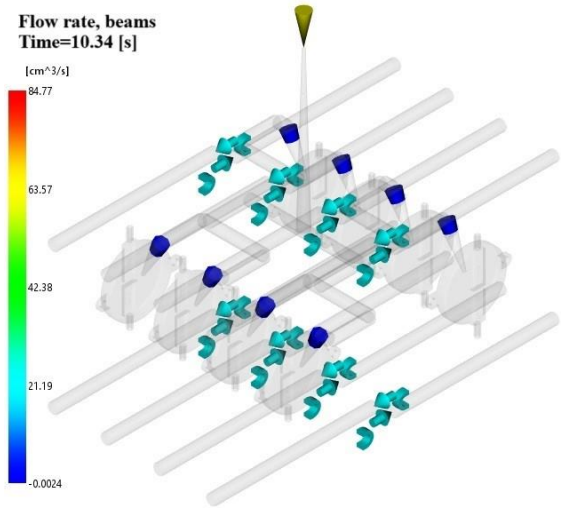

Fig. 8. Flow rate beams analysis results

3.5 Experimental design

This study focuses on how cooling water temperature and flow rate parameters impact product quality and production performance in the injection process. Flow rate effects were evaluated by using the Reynolds number as a key parameter in the flow analysis. The Face-Centered Cubic (FCC) method was used for the Design of Experiments (DOE) in this study. This approach enabled the creation of a comprehensive test setup with systematic combinations based on predefined ranges for cooling water temperature and Reynolds number. Using the optimization module in the program, optimal values for mass production input parameters were statistically determined. Table 3 presents the selected input variables and their respective ranges.

Table 3. Input parameters and boundaries

Input parameter	**Value**
Reynolds Number (m^2/s)	8000-8800
Temperature (°C)	20-30

4. Results

4.1 Circuit presure and metal temperature

The circuit pressure analysis illustrates a uniform and balanced pressure distribution throughout the cooling circuit from inlet to outlet. Figure 9 shows that circuit pressure ranges between 4.517 kPa and 8.648 kPa, depending on the cooling water temperature and Reynolds number. The graph also indicates that lower cooling temperatures and Reynolds numbers lead to reduced circuit pressure.

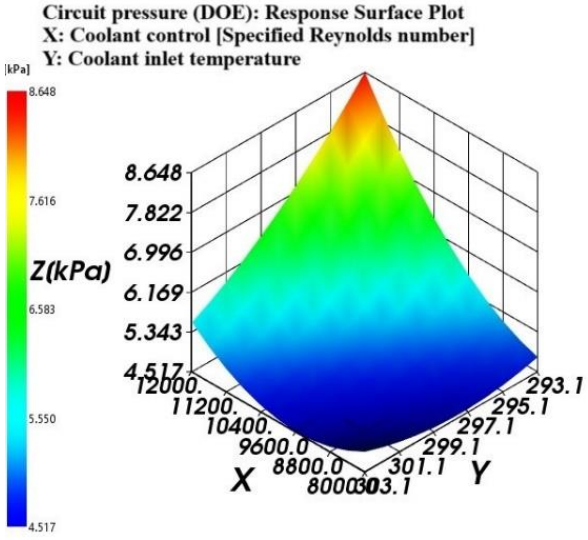

Fig. 9. Circuit pressure results

Metal temperature is a critical factor for managing thermal stresses in the product. Figure 10 shows that, at lower Reynolds numbers and cooling temperatures, the metal temperature follows a similar trend, staying within the 0° to 2.5° range. This indicates that maintaining the metal temperature below 2° is key to minimizing residual stress.

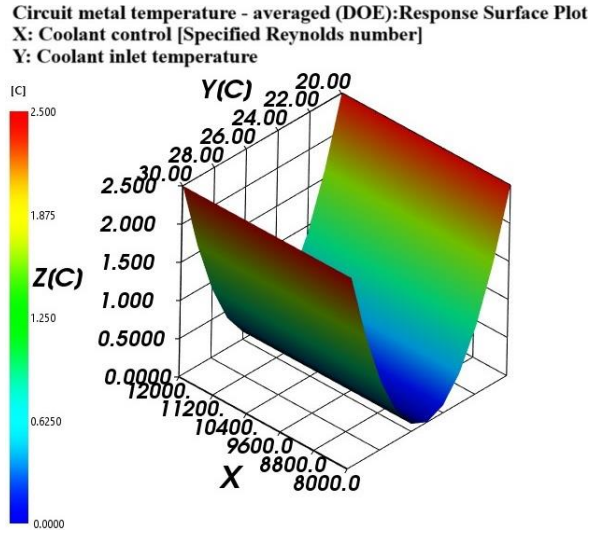

Fig. 10. Circuit metal temperature results

4.2 Bulk temperature and clamp force

Bulk temperature represents the energy transferred across different locations within the material. The polymer melt temperature is influenced by time, position and part thickness, making it challenging to capture all variables in a single measurement. Thus, analyzing bulk temperature is essential. Figure 11 shows that bulk temperature ranges between 6160° and 6284°, clustering around 6215°—an optimal range associated with maximum surface quality.

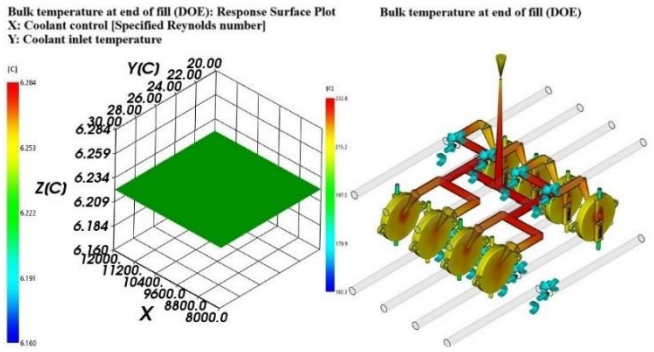

Fig. 11. Bulk temperature at end of fill

Clamp force is the pressure needed to keep the mold closed during injection filling and prevent melt leakage. Figure 12 shows that, despite variations in input parameters, the clamp force remains between 23.51 and 23.89 tonnes, indicating a stable and balanced force throughout the process.

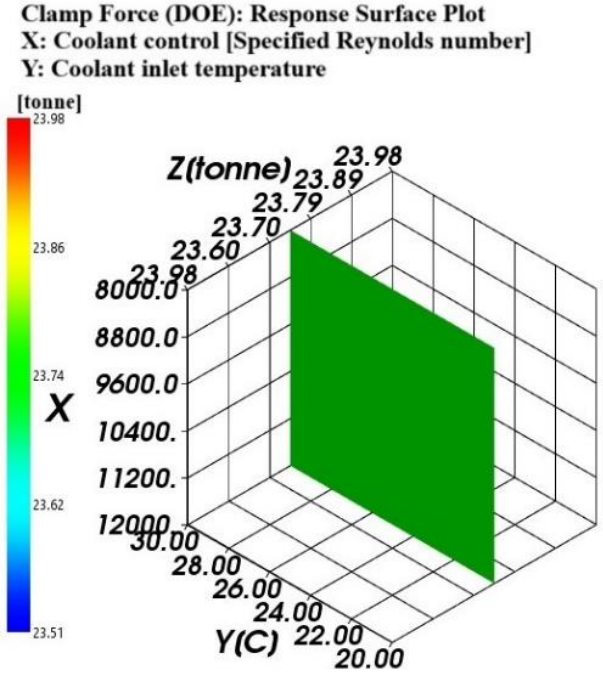

Fig. 12. Clamp force results

4.3 Injection pressure

Injection pressure, generated by the plastic melt at the screw head of the injection machine, overcomes resistance from the nozzle, mold cavity and runner clearance while compressing cavity pressure. As shown in Figure 13, the injection pressure ranges from 113.8 MPa to 116.1 MPa, with an average of 114.9 MPa—an optimal level for effective mold filling and managing stress on the mold.

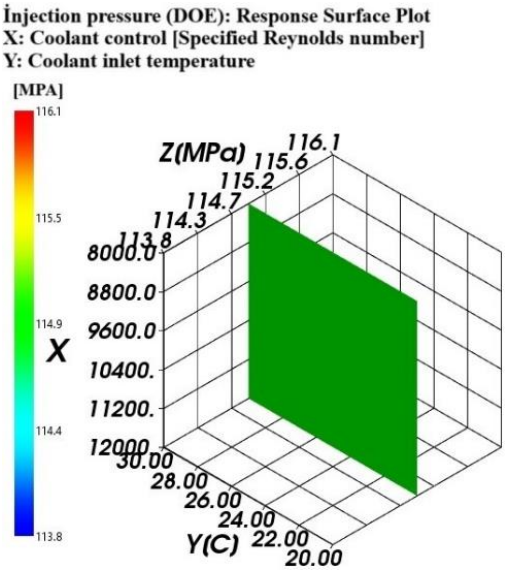

Fig. 13. Injection pressure results

4.4 Wall shear stress and sink mark depth

This parameter reflects the shear stress exerted by molten or solidified plastic on the mold walls, which is closely linked to residual stress and allows for comparison between oriented and non-oriented materials. In oriented materials, shrinkage near the edges tends to be higher, leading to increased residual stress.

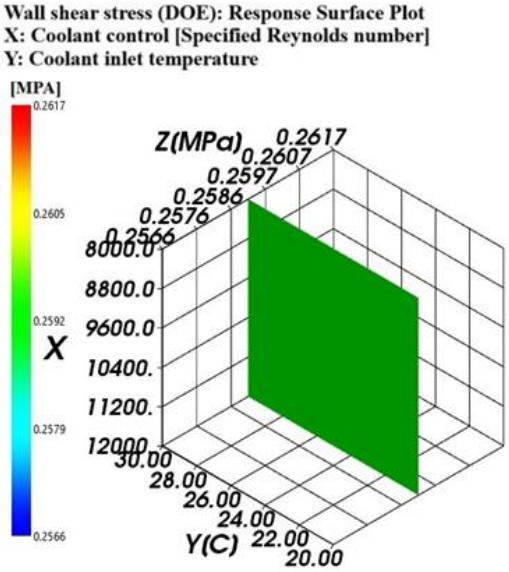

Fig. 14. Wall shear stress results

As shown in Figure 14, shear stress values fall within a low range of 0.2566 MPa to 0.2617 MPa, supporting mold longevity by maintaining stress at an optimal level. Higher shear stress values outside this range could result in mold wear and negatively affect surface quality. Sink mark depth indicates the location and depth of surface depressions. These localized shrinkages can become visible under specific lighting conditions or model colors, potentially impacting product quality. Analysis results (Figure 15) show that sink mark depth remains consistently low, between 0.2995 mm and 0.2999 mm.

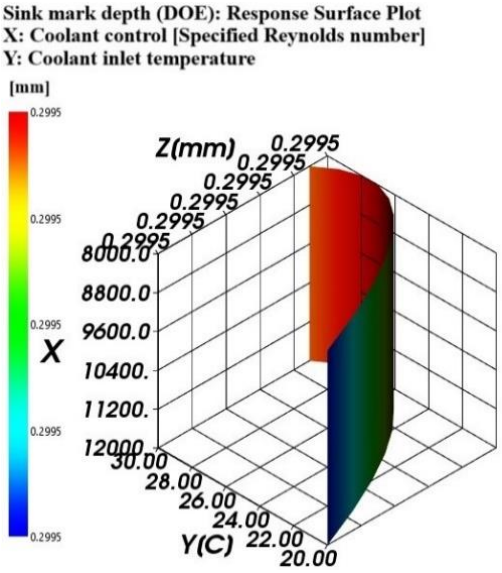

Fig. 15. Sink mark depth results

4.5 Temperature at flow front

This value represents the temperature of the melt at the flow front, which must be kept within a specific range to avoid significant temperature drops. Rapid injection times can cause substantial drops, leading to material degradation or surface defects along the flow direction. Figure 16 shows that this range is between 0.2711°C and 0.2754°C, indicating minimal temperature fluctuations.

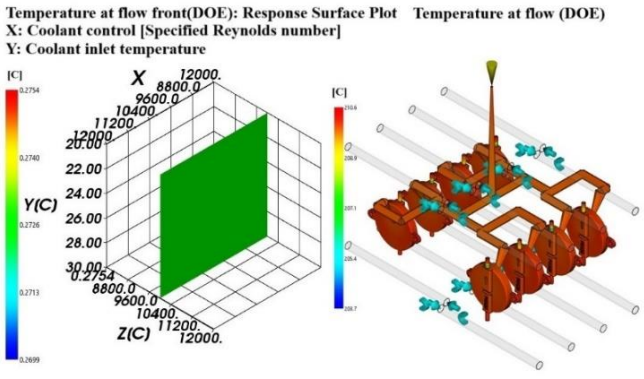

Fig. 16. Temparature at flow front results

4.6 Time distribution and volumetric shrinkage

This value represents the time required to reach ejection temperature from the initial mold filling, which directly affects production time. It is crucial for the entire model to achieve the ejection temperature. As shown in Figure 17, this time ranges within a reasonable 11.15 to 11.58 seconds.

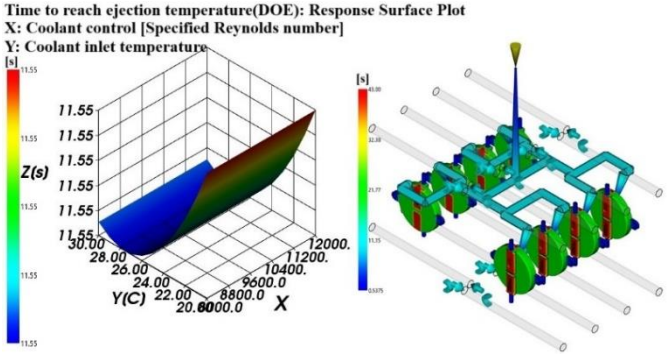

Fig. 17. Time to reach ejection temperature results

This metric represents the dimensional shrinkage ratio across each region of the 3D model, with volumetric shrinkage being essential for maintaining product dimensional accuracy. As shown in Figure 18, a shrinkage rate of 2.775% reflects a high level of product quality.

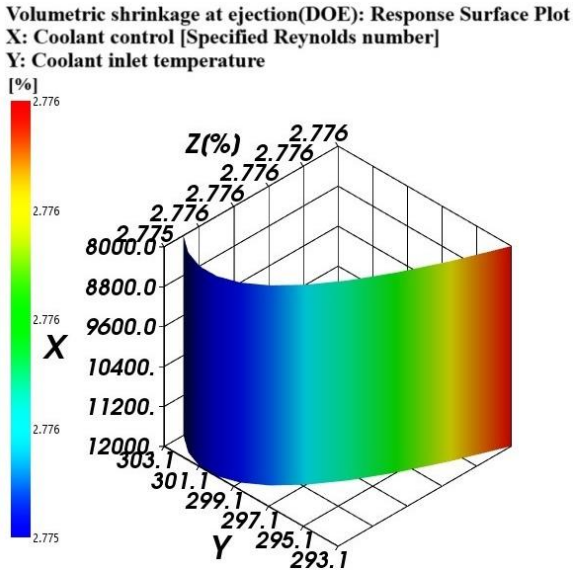

Fig. 18. Volumetric shrinkage at ejection results

4.7 Warpage and fill time

This parameter reflects the final dimensional warpage of the product, as shown in Figure 19. The warpage deformation ranges from 0.0434 mm to 0.0436 mm, indicating that the molded part closely aligns with the dimensions of the 3D model.

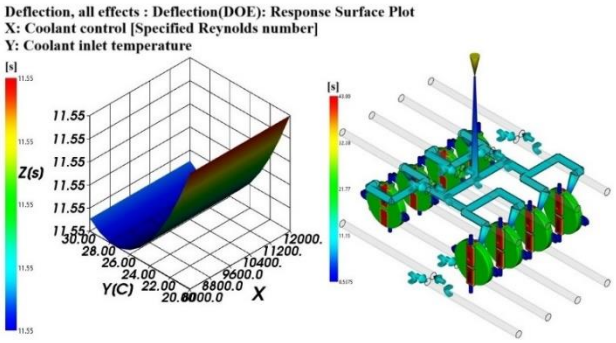

Figure 19. Warpage results

This metric refers to the time required for the melt to fully fill the mold, starting from the injection entry point. While a fast fill time is advantageous, it is also crucial to ensure uniform melt distribution and complete cavity filling. The analysis showed a fill time of 0.3327 seconds. Figure 21 shows the fill time results.

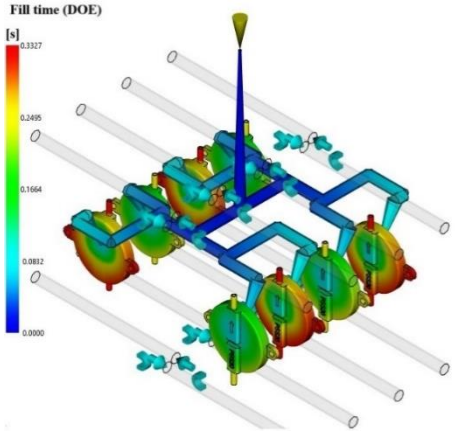

Fig. 20. Fill time results

4.8 Ram speed recommended XY plot

This speed parameter, which maintains the optimal flow rate of the plastic melt, is essential for ensuring fill quality. Figure 21 shows that ram speed is lower at the beginning and end of the fill volume, with an increase observed during the mid-fill phase.

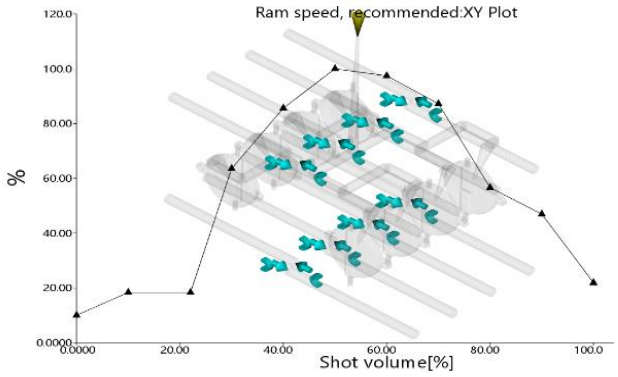

Fig. 21. Ram speed results

5. Conclusion

This study provides an in-depth analysis of how various process parameters impact product quality in the microinjection molding of piezoelectric pumps. Results reveal that key parameters, such as cooling fluid temperature, Reynolds number, have significant effects on the final product's dimensional accuracy, surface quality and mechanical strength.

- Maintaining injection pressure within the range of 113.8 - 116.1 MPa ensured uniform filling and minimized stress within the mold, effectively reducing product deformation. This optimized pressure range not only enhances molding efficiency but also simplifies quality control. A fill time of 0.3327 seconds supported even material distribution and eliminated voids within the mold-essential for maintaining a consistent temperature distribution throughout. Without this, temperature variations could disrupt material flow and compromise product quality. These parameters ensured homogeneous filling and minimized surface deformation.
- Keeping wall shear stress between 0.2566 - 0.2617 MPa helped prevent mold wear and material buildup, extending mold life and improving surface quality. Additionally, stabilizing volumetric shrinkage at 2.775% enhanced product dimensional stability and maintained tight tolerances, a critical factor for high-precision microinjection parts. Moreover, controlling sink mark depth within the range of 0.2995 - 0.2999 mm effectively prevented visible surface imperfections, preserving both aesthetic and functional quality. Dimensional stability was enhanced and these values provided critical data for the production of precise microinjection-molded products.
- Maintaining the cooling water temperature between 20-30°C enhanced product quality in microinjection production while also extending the lifespan of the injection mold. The impact of cooling water temperature, one of the key injection parameters, on product quality has been investigated in Wu-lin Chen's study [15] to minimize volumetric shrinkage and warpage. However, this study further demonstrates that maintaining the cooling water temperature within the range of 20-30°C exerts a precise effect on both filling time and surface deformations. In doing so, it contributes significantly to the literature on microinjection processes.
- H.K. Lee's study [16] on residual stress analysis for thin-walled polymers in the context of microinjection processes required validation through photoelastic methods. However, this study establishes a direct and measurable relationship by optimizing surface deformations, offering a more concrete and practical approach. This significantly enhances the applicability and relevance of the results.
- Literature studies primarily focus on the molding process of automotive parts, with an emphasis on filling time and mechanical properties. In this study, however, the effects of cooling parameters, particularly the Reynolds number, on injection pressure and surface quality were analyzed, highlighting the influence of different operational parameters.
- Together, these parameters demonstrate the advantages of optimizing microinjection molding settings for piezoelectric pump production, boosting both quality control and production efficiency. Future research could further examine these parameters' effects on complex microstructures, setting new standards for efficiency and quality in microinjection processes. These insights provide valuable guidance not only for piezoelectric pump manufacturing but also for producing other high-precision micro-components.

Conflict of Interest Statement

The authors declare that there is no conflict of interest in the study.

CRediT Author Statement

Fuat Tan: Writing-original draft, Supervision, Analysis, Validation, **Ahmet Kerem Alkan**: Numerical Analysis, Data curation

References

[1] V. Piotter, W. Bauer, T. Benzler, A. Emde. Injection molding of components for microsystems. Microsystem Technologies. 2001; 7: 99-102.

[2] Fu H, Xu H, Liu Y, Yang Z, Kormakov S, Wu D, Sun J. Overview of injection molding technology for processing polymers and their composites. ES Materials & Manufacturing.2020; 8(20): 3-23. https://doi.org/10.30919/esmm5f713

[3] Dekel Z, Kenig S. Micro-injection molding of polymer nanocomposites composition-process-properties relationship. International Polymer Processing. 2021; 36(3): 276-286. https://doi.org/10.1515/ipp-2020-4065

[4] Bellantone V, Surace R, Fassi I. Quality definition in micro injection molding process by means of surface characterization parameters. Polymers. 2022; 14(18): 3775. https://doi.org/10.3390/polym14183775

[5] Speranza V, Liparoti S, Pantani R, Titimanlio G. Prediction of morphology development within micro–injection molding samples. Polymer. 2021; 228:123850. https://doi.org/10.1016/j.polymer.2021.123850

[6] Gal CW, Han JS, Park JM, Kim JH, Park SJ. Fabrication of micro piezoelectric rod array using metallic mold system for mass production. The International Journal of Advanced Manufacturing Technology. 2019;101:2815–2823. https://doi.org/10.1007/s00170-018-2986-6

[7] Tuckerman D, Pease R. High-performance heat sinking for VLSI. IEEE Electron Device Letters. 1981;2(5):126–129. https://doi.ogr/ 10.1109/EDL.1981.25367

[8] Manz A, Harrison DJ, Verpoorte EMJ, Fettinger JC, Paulus A, Lüdi H, Widmer HM Planar chips technology for miniaturization and integration of separation techniques into monitoring systems—capillary electrophoresis on a chip. J. Chromatography A. 1992;593 (1-2):253–258. https://doi.org/10.1016/0021-9673(92)80293-4

[9] Kulkarni H, Zohaib K, Khusru A, Aiyappa KS. Application of piezoelectric technology in automotive systems. Materials Today: Proceedings. 2018; 5(10): 21299-21304. https://doi.org/10.1016/j.matpr.2018.06.532

[10] Chang HT, Wen CY, Lee CY. Design, analysis and optimization of an electromagnetic actuator for a micro impedance pump. Journal Of Micromech. Microeng. 2009;19(8):85026. https://doi.org/10.1088/0960-1317/19/8/085026

[11] Li X, Lİ D, Liu X, Chang H. Ultra-monodisperse droplet formation using PMMA microchannels integrated with low-pulsation electrolysis micropumps. Sensors and Actuators B. 2016;229:466–475. https://doi.org/10.1016/j.snb.2016.01.122

[12] Chang HT, Lee CY, Wen CY. Design and modeling of electromagnetic actuator in mems-based valveless impedance pump. Microsystem Technologies. 2007;13:1615–1622. https://doi.org/10.1007/s00542-006-0332-7

[13] Yeo HG, Jung J, Sim M, Jang JE, Choi H. Integrated piezoelectric AIN thin film with SU-8/PDMS supporting layer for flexible sensor array. Sensors.2020;20(1):315. https://doi.org/10.3390/s20010315

[14] Karaağaç İ, Uluer O, Gürün H, Mert F. Plastik Enjeksiyon Kalıplarında Maliyet Tahmini. In 1st International Symposium on Plastic and Rubber Technologies and Exhibition. 2013; 29-40.

[15] Schulze R, Heinrich M, Nossol P, Forke R, Sborikas M, Tsapkolenko A, Billep D, Wegener M, Kroll L, Gessner, T. Piezoelectric P (VDF-TrFE) transducers assembled with micro injection molded polymers. Sensors and Actuators A: Physical. 2014;208:159-165. https://doi.org/10.1016/j.sna.2013.12.032

[16] Wegener M, Künstler W, Richter K, Gerhard-Multhaupt R. Ferroelectric polarization in stretched piezo- and pyroelectric poly (vinylidene fluoride-hexafluoropropylene) copolymer films.Journal of Applied Physics. 2002; 92 (12):7442-7447. https://doi.org/10.1063/1.1524313

[17] Arlt K, Wegener M. Piezoelectric PZT / PVDF-copolymer 0-3 composites; Aspects on film preparation and electrical poling. IEEE Transactions on Dielectrics Electrical Insulation. 2010;17(4):1178-1184. https://doi.org/10.1109/TDEI.2010.5539688

[18] Wegener M, Bauer S. Microstorms in cellular polymers: A route to soft piezoelectric transducer materials with engineered macroscopic dipoles. Chem. Phys. Chem.2005;66: 1014-1025. https://doi.org/10.1002/cphc.200400517

[19] Chen WL, Huang CY, Hung CW, Optimization of plastic injection molding process by dual response surface method with non-linear programming. International Journal for Computer-Aided Engineering and Software. 2009;27(8):951-996.

[20] Lee HK, Huang JC, Yang GE, Kim HG. Analysis of residual stress in thin wall injection molding. Key Engineering Materials. 2006;306:1331-1336. https://doi.org/10.4028/www.scientific.net/KEM.306-308.1331

[21] Zheng G, Guo W, Wang Q, Guo X. Influence of processing parameters on warpage according to the Taguchi experiment. Journal of Mechanical Science and Technology. 2015; 29(10):4153-4158. https://doi.org/10.1007/s12206-015-0909-0

[22] Tosello G, Costa FS. High precision validation of micro injection molding process simulations. Journal of Manufacturing Processes. 2019;48: 236-248. https://doi.org/10.1016/j.jmapro.2019.10.014

[23] Wu HL, Wang YH. Using taguchi method to optimize Molding Process Parameters of Chair Base. Applied Mechanics and Materials. 2013; 271:1190-1194. https://doi.org/10.4028/www.scientific.net/AMM.271-272.1190

[24] Bharti PK, Khan MI. Recent methods for optimization of plastic injection molding process-A retrospective and literature review. International Journal of Engineering Science and Technology. 2010;2(9):4540-4554.

[25] Fu JY. The viscosity model of Ti-6Al-4V feedstocks in metal powder injection molding. Applied Mechanics and Materials. 2013;.275: 2161-2165. https://doi.org/10.4028/www.scientific.net/AMM.275-277.2161

[26] Qian YP, Wang Y, Huang JH, Zhou XZ. Study on the optimization of conformal cooling channels for plastic injection mold. Advanced Materials Research. 2012; 591: 502-506. https://doi.org/10.4028/www.scientific.net/AMR.591-593.502

[27] Huang ZM, Kim HM, Youn JR, Song YS. Injection molding of carbon fiber composite automotive wheel. Fibers and Polymers. 2019; 20: 2665-2671. https://doi.org/10.1007/s12221-019-9636-y

[28] Wang G, Wang Y, Yang D. Study on automotive back door panel injection molding process simulation and process parameter optimization. Advances in Materials Science and Engineering. 2021;(1): 9996423. https://doi.org/10.1155/2021/9996423

[29] Yang H, Jo H, Lee H, Park, H, Park J. A New Approach to Optimization of the Injection Molding on Automotive Interior Parts. SAE Technical Paper.2016; 1:3-6. https://doi.org/10.4271/2016-01-0306

[30] Spina R. Injection moulding of automotive components: comparison between hot runner systems for a case study. Journal of Materials Processing Technology. 2004; 155 :1497-1504. https://doi.org/10.1016/j.jmatprotec.2004.04.359

[31] Park HS, Dang XP. Development of a smart plastic injection mold with conformal cooling channels. Procedia Manufacturing. 2017;10: 48-59. https://doi.org/10.1016/j.promfg.2017.07.020

[32] Jauernick M, Schütz C, Sterz J, Horn B. Composite Engine Block–Challenges for Design and Material. Technologies for economical and functional lightweight design. 2019; 51-60. https://doi.org/10.1007/978-3-662-58206-0_5